High-resolution photoelectron spectroscopy of linear bent polyatomic photodetachment transitions: The electron affinity of CS2

S. J. Cavanagh, S. T. Gibson, and B. R. Lewis

Citation: The Journal of Chemical Physics **137**, 144304 (2012); doi: 10.1063/1.4757726
View online: http://dx.doi.org/10.1063/1.4757726
View Table of Contents: http://scitation.aip.org/content/aip/journal/jcp/137/14?ver=pdfcov
Published by the AIP Publishing

High-resolution photoelectron spectroscopy of linear ← bent polyatomic photodetachment transitions: The electron affinity of CS_2

S. J. Cavanagh, S. T. Gibson, and B. R. Lewis
Research School of Physics and Engineering, The Australian National University, Canberra, ACT 0200, Australia

(Received 23 July 2012; accepted 24 September 2012; published online 10 October 2012)

A combination of high-resolution velocity-map-imaging photoelectron spectroscopy and isotopic substitution is used to show that precise electron affinities can be obtained from polyatomic photodetachment spectra, even for cases involving significant changes in equilibrium geometry between the molecular neutral and anion. The chosen example CS_2 $(X\,^1\Sigma_g^+)$ (linear) ← CS_2^- $(X\,^2A_1)$ (bent) photodetachment transition is found to preferentially access highly-excited v_2 (bending) levels of the neutral, with no observation possible of the lowest-v_2 bands. Nevertheless, through ^{13}C isotopic substitution, the v_2 numbering is established unambiguously and the adiabatic electron affinity of CS_2 is found to be 4456(10) cm^{-1} [0.5525(13) eV], by far the most precise value reported to date. © *2012 American Institute of Physics*. [http://dx.doi.org/10.1063/1.4757726]

The electron affinity (EA) is an important physical property of atoms, molecules, and radicals, representing the difference in energy between the neutral species and the negative ion resulting from its binding of an additional electron. In addition to the fundamental significance of EAs in atomic and molecular physics and gas-phase ion chemistry, the properties of negative ions are also of importance in many other subfields of pure chemistry, materials science, environmental chemistry, biochemistry, and biology, as evidenced, e.g., by the specific examples cited in a major review on the subject.[1] The most accurate general method of measuring EAs is threshold photodetachment spectroscopy, in which the appearance energy of photoelectrons following the irradiation of anions with tunable laser radiation can be determined precisely to a level controlled essentially by the laser bandwidth. However, for larger and more complex ions, it is difficult to determine the threshold for electron detachment accurately using this technique, especially for other than *s*-wave photodetachment, and laser photoelectron spectroscopy (LPES) is commonly employed. In this variant, the laser frequency is fixed and the kinetic-energy spectrum of the photodetached electrons is measured, albeit at a lower resolution controlled by the characteristics of the electron spectrometer. The various experimental methods used for anion photoelectron spectroscopy have been well reviewed recently by Neumark,[2] including several high-resolution variants such as photodetachment microscopy,[3] zero electron kinetic-energy spectroscopy,[4] and slow electron velocity-map imaging,[5] all of which are capable of precision measurement, but only over very limited ranges of electron kinetic energy (eKE).

In the case of a molecular target where the lowest vibrational level of the neutral is readily accessed in the photodetachment transition, the EA can be measured directly using LPES. However, in cases where poor Franck-Condon overlap due to a significant difference in equilibrium geometry between the anion and neutral mandates that only highly-excited neutral levels are accessed, then only an extrapolated EA may be determined. Nevertheless, as will be demonstrated here, provided that the vibrational levels of the neutral are well characterized and their numbering in the photoelectron spectrum can be established unambiguously, then even in these cases, the EAs can be determined with normal LPES precision.

Here, we use CS_2 as the target triatomic, representative of the above molecular class. Whereas the neutral $CS_2(X\,^1\Sigma_g^+)$ molecule is linear, the corresponding anion, $CS_2^-(X\,^2A_1)$, is bent, leading to poor Franck-Condon overlap in the vertical photodetachment transition and a long progression in the bending (v_2) vibration with no clear origin. Experimental values for the EA of CS_2, determined using a variety of techniques, range from $\sim 0.5 - 1.0$ eV,[6] indicating significant uncertainty. More recent *ab initio* calculations[7–9] lie in the ∼0.30–0.54-eV range, favouring the lower experimental determinations. LPES has been of limited utility in elucidating the EA of CS_2,[9–14] compromised, not only by the poor Franck-Condon overlap, but also by limited resolution in the anion photoelectron spectra. From vibrationally-resolved photodetachment spectra, Oakes and Ellison,[11] noting the difficulty of locating the lowest-v_2 band, deduced an EA of 0.895(20) eV, while Schiedt and Weinkauf[12] found an upper limit of 0.8 eV. Finally, Misaizu *et al.*[9] estimated an EA of 0.58(5) eV from the "threshold" of a vibrationally-unresolved spectrum. Considering the lack of convincing vibrational assignment for the partially-resolved spectra, and the arbitrary nature of the threshold estimation for the unresolved case, it appears that the only definitive conclusion from the previous LPES results is that EA $\leq$0.8 eV.

In the present work, we use high-resolution LPES to fully resolve the CS_2 $(X\,^1\Sigma_g^+)$ ← CS_2^- $(X\,^2A_1)$ photodetachment transition vibrational structure, together with ^{13}C isotopic substitution to aid in vibrational assignment, resulting in the first accurate LPES determination of the EA for CS_2. The high-resolution photodetachment spectrometer employed has been described in detail elsewhere.[15,16] Briefly, a collimated

beam of mass-selected anions was produced and crossed by a laser beam, generating photoelectrons which were imaged using a velocity-mapped imaging (VMI) lens onto a multichannel plate (MCP) and phosphor detector. Ar gas was passed over a liquid source of $^{12}CS_2$ and $^{13}CS_2$ (3:1 ratio), the consequent vapor carried through a pulsed nozzle at a stagnation pressure of 2.6 atm and then supersonically expanded through a pulsed electrical discharge, producing an isotopic mixture of CS_2 anions, which were then extracted, accelerated to 500 eV, gated, bunched, and passed through a 2-m time-of-flight (TOF) tube. Following mass selection with a potential barrier, the anions entered a coaxially-mounted VMI lens. This is a substantially modified version of the Eppink and Parker original,[17] designed specifically to accommodate fast ion beams and large interaction volumes while simultaneously achieving very high eKE resolution. The detachment laser beam, with a bandwidth of 0.08 cm^{-1} and pulse energies in the range 1–3 mJ, was provided by an optical parametric oscillator (OPO) pumped by the 355-nm third harmonic of a Nd:YAG laser operated at 10 Hz. It was reduced to a parallel beam 2 mm in diameter before entering the VMI lens and, to ensure a high degree of polarization parallel to the MCP detector face, was passed through a half-wave plate and broad-bandwidth Glan-Laser polarizer. The output wavelength of the OPO was monitored during the course of the measurements by a wave meter. Photoelectrons were imaged onto the MCP-phosphor detector, located at the end of a TOF tube 800 mm from the interaction region, with magnetic field screening achieved by a combination of μ-metal shielding and orthogonal Helmholtz coils. The MCP gain was gated to ensure that unwanted events from untargeted ions and neutral species were not detected.

Images from the phosphor were captured by a CCD camera and processed in real time to centroid each event to subpixel accuracy. In order to extract the 3D distribution from the 2D image, an inverse Abel transformation was performed, using the method of Hansen and Law.[18] However, for optimum eKE resolution, it was first necessary to remove the small (~1%) image distortion by using a circularization procedure based on the comparison of radial image slices. Energy calibration was achieved using S^- photodetachment, since the spectroscopies of both the anion and the neutral are well known. Using optimum voltages and a stable ion beam, eKE resolving powers of $\Delta E/E = 0.2\%$–0.3% were achieved typically.

VMI results for the 800.88 nm photodetachment of $^{12}CS_2^-$ are shown in Fig. 1; the left-hand side showing the raw experimental image, following circularization, the right-hand side the inverted image from the corresponding Abel transformation. In Fig. 1, the horizontal axis corresponds to the direction of the laser beam, the vertical axis to the polarization direction, and the image center to the photodetachment threshold (zero eKE). It is clear from the inverted image that the vibrational structure is fully resolved. Furthermore, while the photoelectron angular distribution is tending towards isotropic near threshold, there is significant anisotropy above threshold, observations consistent with the previous VMI study of Surber *et al.*[13,14] In the present work, we are concerned principally with the photodetachment spectrum and therefore defer the further discussion of angular distributions to another paper.[19]

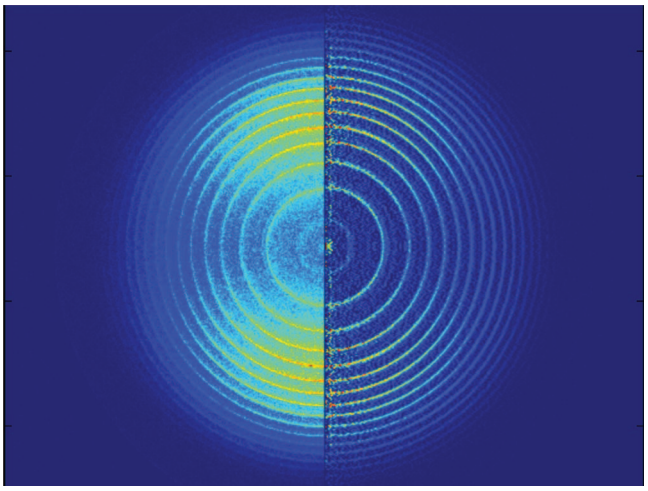

FIG. 1. (Left side) VM image for 800.88 nm photodetachment of $^{12}CS_2^-$ (~6×10^6 photoelectrons binned to a 1024 × 1024 pixel image). (Right side) Corresponding 3D-slice image, from the inverse Abel transformation.

The $^{12}CS_2^-$ photoelectron spectrum extracted from the data in Fig. 1 is shown in Fig. 2 (black curve), as a function of the electron binding energy, eBE = $h c \nu$ −eKE, where ν is the wave number for the photodetachment laser.[20] The broad features of the spectrum agree with those displayed in the corresponding, but much lower-resolution spectrum of Surber and Sanov (Fig. 2 of Ref. 13), i.e., a long progression of peaks with roughly equal spacings of ~420 cm^{-1}, consistent with the bending vibrational quantum in neutral CS_2, ω_2 = 398 cm^{-1},[21] and, therefore, with an assignment to a transition from the bent ground state of CS_2^- to excited bending levels of the linear CS_2 ground state. However, in addition, the very high resolution of the present spectrometer leads to the first observation of subband structure in CS_2^- photodetachment, most clearly evidenced by alternating peak heights in the vibrational structure in Fig. 2. On closer examination, one set of peaks (type a) comprises close doublets, of similar intensity and separated by ~30 cm^{-1}, while the alternate set (type b) consists of a strong single peak, with a weaker companion situated ~64 cm^{-1} towards lower eBE. If the integrated peak intensities are summed over the subbands within a given vibrational band, then the apparent intensity alternation disappears, explaining the lack of observation of such alternation in all previous low-resolution spectra. The structure observed in the present spectrum, including the subband alternation, is similar to that observed in the linear ← bent vacuum-ultraviolet absorption spectrum of NO_2,[22] a molecule isoelectronic with CS_2^-.

To determine the EA of CS_2 from the present measurements, it is necessary first to consider some aspects of the rotational structure of the CS_2 ($X\,^1\Sigma_g^+$) ← CS_2^- ($X\,^2A_1$) photodetachment transition. In its doublet bent ground state, the asymmetric-top CS_2^- molecule may be viewed as a prolate symmetric top, with rotational energy levels in the rigid-rotor approximation given by

$$E(N, K) = \bar{B}N(N+1) + (A - \bar{B})K^2, \quad (1)$$

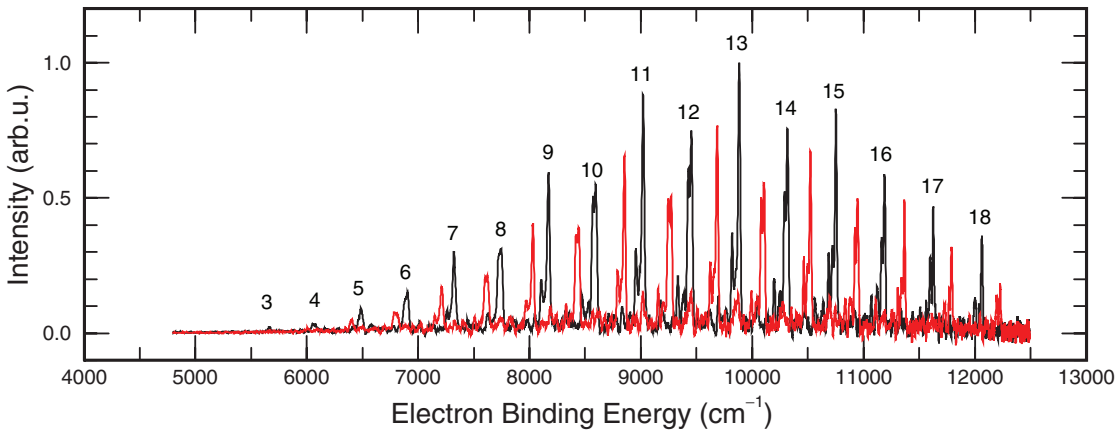

FIG. 2. High-resolution photoelectron spectra for the photodetachment of CS_2^- at 800.88 nm, as a function of eBE. Black curve: $^{12}CS_2$. Red curve: $^{13}CS_2$. The $^{12}CS_2$ peaks are labelled with the bending vibrational quantum number of the neutral ground state. Both spectra show alternating substructure: type-a peaks, for v_2' even; type-b, for v_2' odd (see text).

where N and K are the quantum numbers for the total angular momentum (exclusive of spin) and its well-defined component about the figure axis, respectively, $\bar{B} = (B + C)/2$, and $A \gg B \approx C$ are the rotational constants associated with the orthogonal symmetry axes.[23] Thus, the (0,0,0) initial vibrational level for the photodetachment transition supports a $K = 0$, 1, 2… substructure with quadratically increasing spacing, with each K-sublevel supporting closely-spaced rotational structure. Even at low temperatures, several K-sublevels are expected to be populated. In the case of the linear $^1\Sigma_g^+$ ground state of CS_2, the final state of the photodetachment transition, the degenerate bending vibrational levels support a substructure labelled by the vibrational angular-momentum quantum number $l = 0, 2, 4, \ldots, v_2$, for even v_2 ($l = 1, 3, 5, \ldots, v_2$, for odd v_2), leading to an l-substructure of increasing complexity as v_2 increases, each l-sublevel supporting closely-spaced rotational structure. In the case of excited bending levels, as we have here, the singlet CS_2 ground state may also be treated as a prolate symmetric top, with rotational energy levels given by Eq. (1), but with $N = J$, $\bar{B} = B$, $K = l$, and the effective constant A much smaller than for the bent CS_2^- ground state. Thus, the linear ← bent photodetachment transition is expected to exhibit a number of $K' \leftarrow K''$ subbands, which diverge strongly towards lower eBE. If $\Delta K = 0$, subbands with even or odd K'' will be missing for odd or even v_2', respectively, and for even or odd v_2', respectively, if $\Delta K = \pm 1$. Specific band structures for these cases have been given in Fig. 90 of Ref. 23, for optical transitions. Analysis of the strongest peaks in Fig. 2 confirms that the observed subband structure is consistent only with $\Delta K = 0$:[24] the type-a structure has v_2' even, containing the closely-spaced $K' = 0 \leftarrow K'' = 0$ and $K' = 2 \leftarrow K'' = 2$ subbands, the latter to lower eBE; the type-b structure has v_2' odd, containing the strong $K' = 1 \leftarrow K'' = 1$ and weaker $K' = 3 \leftarrow K'' = 3$ subbands. It is the $v_2' = 0$ limit of the $K' = 0 \leftarrow K'' = 0$ subband eBEs, which defines the adiabatic EA.

The nearly equal spacing of the v_2' levels militates against vibrational assignment using energy spacings alone, even given the extra discrimination provided by the alternating subband structure. Therefore, isotopic substitution has been employed to aid the assignment. The photoelectron spectrum for $^{13}CS_2^-$ photodetachment, extracted from a VM image recorded on the same day using exactly the same conditions, calibration, and circularization procedure as for the $^{12}CS_2^-$ case, is shown as the red curve in Fig. 2. The peaks for the heavier isotopomer are displaced to lower eBE, by a smaller amount as v_2' decreases. Magnitudes of the isotopic shifts[25] determined from the $K' = 0 \leftarrow K'' = 0$ subbands in Fig. 2 are shown as the solid circles in Fig. 3, plotted assuming the nominal v_2' assignment of Fig. 2.

Isotopic shifts for the lower levels of the CS_2 ($X\,^1\Sigma_g^+$) state are known precisely from experiment[26] and have been successfully modelled theoretically.[27] However, in order to compare these level shifts with the subband shifts in Fig. 3,

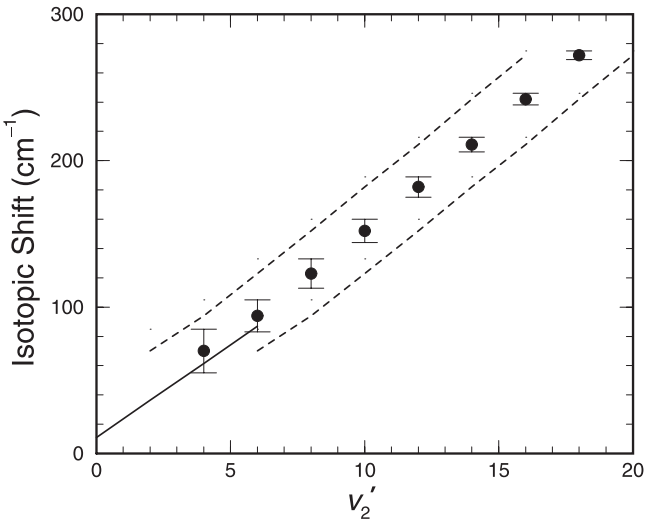

FIG. 3. Isotopic shifts for the $K' = 0 \leftarrow K'' = 0$ subbands in the $(0, v_2', 0) \leftarrow (0, 0, 0)$ photodetachment transition. Solid circles: Present results from spectra in Fig. 2, with nominal vibrational assignment. Dashed curves: Present results shifted by ±2 vibrational units. Solid curve: Shifts for $(0, v_2', 0)$ (Ref. 27), shifted up by estimated ZPE shift (see text).

it is necessary first to estimate and correct for the isotopic shift in the zero-point-energy (ZPE) transition. Using the CS_2 and CS_2^- vibrational frequencies and structures calculated by Shao *et al.*[28] at the same theoretical level, and assuming the harmonic approximation, the ZPE isotopic shift is found to be $\sim$11 cm^{-1}. The solid curve in Fig. 3, representing the isotopic level shifts of Zhou *et al.*,[27] raised by 11 cm^{-1}, is in good agreement with the trend of the present subband shifts (solid circles), but not with those implied by shifts in v_2' of ± 2 units (dashed curves). Since the anion ground state is expected to be more anharmonic than that of the neutral,[7] the true ZPE shift will likely be $>$11 cm^{-1}, resulting in even better agreement. Thus, the correct vibrational numbering is established as that shown in Fig. 2.

Using this numbering, together with the known energy spacings for the $(0, v_2', 0)$ levels with $l' = K' = 0$ from the work of Zhou *et al.*,[27] it is now possible to recalibrate the energy scale for the experimental spectra, which was originally based on a nonsimultaneous S^- calibration. Indeed, it is these recalibrated spectra that are plotted in Fig. 2. Fortunately, the recalibration results in a change of only 0.2% in the energy scale factor, compared with -0.8% and 1.1%, respectively, for the $v_2' - 2$ and $v_2' + 2$ numbering choices. Using the $K' = 0 \leftarrow K'' = 0$ recalibrated subband eBEs, and subtracting the corresponding $(0, v_2', 0)$ level energies,[27] leads to an accurate determination of the EA for CS_2. The average result obtained from the $v_2' = 4, 6, \ldots, 18$ subbands is 4456 cm^{-1}. The 3 cm^{-1} peak-to-peak variability in this result is consistent with expectation for the determination of peak energies from spectra with effective peak widths ranging from $\sim$10–30 cm^{-1} at high and low eBE, respectively.[29] However, the *J*-rotational structure is not resolved experimentally and is only partially allowed for in the recalibration procedure. Accordingly, we increase the uncertainty estimate for the EA to allow for rotational-structure effects and determine a final result of 4456(10) cm^{-1} [0.5525(13) eV]. Our EA is 15$\times$ more precise than claimed for any previous experimental determination and supports the lower range of previous experimental results and the higher range of recent theoretical calculations.

Furthermore, the technique employed here may be applicable to the accurate determination of EAs for other polyatomic molecules having linear $\leftarrow$ bent photodetachment transitions, provided that the neutral vibrational structure is well characterized and enough information exists to enable an estimate of the ZPE isotopic shift to be made. In these cases, high-resolution LPES provides an efficient experimental method, covering the associated long vibrational progressions in a single scan.

This research was supported by the Australian Research Council (Grant Nos. DP0666267 and DP0880850). The authors thank A. Sanov and R. Mabbs for comments on the manuscript.

[1] J. C. Rienstra-Kiracofe, G. S. Tschumper, H. F. Schaefer III, S. Nandi, and G. B. Ellison, Chem. Rev. **102**, 231 (2002).
[2] D. M. Neumark, J. Phys. Chem. A **112**, 13287 (2008).
[3] C. Blondel, C. Delsart, and F. Dulieu, Phys. Rev. Lett. **77**, 3755 (1996).
[4] T. N. Kitsopoulos, I. M. Waller, J. G. Loeser, and D. M. Neumark, Chem. Phys. Lett. **159**, 300 (1989).
[5] J. Zhou, E. Garand, and D. M. Neumark, J. Chem. Phys. **127**, 114313 (2007).
[6] NIST Standard Reference Database 69: *NIST Chemistry WebBook*.
[7] G. L. Gutsev, R. J. Bartlett, and R. N. Compton, J. Chem. Phys. **108**, 6756 (1998).
[8] S. Barsotti, T. Sommerfeld, M.-W. Ruf, and H. Hotop, Int. J. Mass. Spectrom. **233**, 181 (2004).
[9] F. Misaizu, H. Tsunoyama, Y. Yasumura, K. Ohshimo, and K. Ohno, Chem. Phys. Lett. **389**, 241 (2004).
[10] T. Tsukuda, T. Hirose, and T. Nagata, Chem. Phys. Lett. **279**, 179 (1997).
[11] J. M. Oakes and G. B. Ellison, Tetrahedron **42**, 6263 (1986).
[12] J. Schiedt and R. Weinkauf, Chem. Phys. Lett. **274**, 18 (1997).
[13] E. Surber and A. Sanov, J. Chem. Phys. **116**, 5921 (2002).
[14] E. Surber, R. Mabbs, and A. Sanov, J. Phys. Chem. A **107**, 8215 (2003).
[15] S. J. Cavanagh, S. T. Gibson, M. N. Gale, C. J. Dedman, E. H. Roberts, and B. R. Lewis, Phys. Rev. A **76**, 052708 (2007).
[16] R. Mabbs, F. Mbaiwa, J. Wei, M. Van Duzor, S. T. Gibson, S. J. Cavanagh, and B. R. Lewis, Phys. Rev. A **82**, 011401(R) (2010).
[17] A. T. J. B. Eppink and D. H. Parker, Rev. Sci. Instrum. **68**, 3477 (1997).
[18] E. W. Hansen and P.-L. Law, J. Opt. Soc. Am. A **2**, 510 (1985).
[19] S. J. Cavanagh, S. T. Gibson, B. R. Lewis, R. Mabbs, and A. Sanov, "High-resolution photodetachment spectroscopy of the carbon disulfide anion," J. Chem. Phys. (to be published).
[20] Because of the high resolution of the present spectra, we use cm^{-1} units for energy.
[21] G. Brasen and W. Demtröder, J. Chem. Phys. **110**, 11841 (1999).
[22] R. K. Ritchie and A. D. Walsh, Proc. R. Soc. London, Ser. A **267**, 395 (1962).
[23] G. Herzberg, *Molecular Spectra and Molecular Structure III. Electronic Spectra and Electronic Structure of Polyatomic Molecules* (Van Nostrand, Princeton, 1966), pp. 82–84 and 209–213.
[24] Some weaker features are consistent with $\Delta K = \pm 1$: Discussion of these subbands is deferred to Ref. 19.
[25] $^{13}C-^{12}C$ isotopic shifts for the photodetachment transition and its initial and final levels are all *negative*. In the text, it is the magnitude of such shifts, which is discussed.
[26] J. Walrand, V. Humblet, and G. Blanquet, J. Mol. Spectrosc. **127**, 304 (1988).
[27] C. Zhou, D. Xie, R. Chen, G. Yan, H. Guo, V. Tyng, and M. E. Kellman, Spectrochim. Acta, Part A **58**, 727 (2002).
[28] L. Shao, M. Chen, and M. Zhou, J. Mol. Struct. **542**, 57 (2001).
[29] At high eBE, the observed peak widths are limited by the unresolved *J*-rotational structure.